Mixed Controller Design for Multi-Vehicle Formation Based on Edge and Bearing Measurements

Kefan Wu, *Student Member, IEEE*, Junyan Hu, *Member, IEEE*, Barry Lennox, *Senior Member, IEEE*, and Farshad Arvin, *Senior Member, IEEE*

***Abstract*— Inspired by natural swarm collective behaviors such as colonies of bees and schools of fish, coordination strategies in swarm robotics have received significant attention in recent years. In this paper, a mixed formation control design based on edge and bearing measurements is proposed for networked multi-vehicle systems. Although conventional edge-based controllers have been widely used in many formation tasks, the tracking accuracy may not be guaranteed in some extreme environments as it depends on the quality of the sensors and requires the exact position data of each vehicle. To overcome this limitation, we combine the edge-based controller with a bearing-based method where only relative bearings among the vehicles are required. Depending on the sensing-ability of the robotic platform, this mixed control method can provide an efficient solution to maximise the tracking performance. Both leaderless and leader-follower cases are considered in the protocol design. The stability of the networked multi-vehicle systems under the proposed mixed formation approach is ensured by Lyapunov theory. Finally, we present simulation results to verify the effectiveness of the theoretical results.**

I. Introduction

Research on cooperative control in multi-vehicle systems (MVSs) has attracted increasing attention over the past decade. Many real-world applications have been explored by researchers, such as drone formation-flying [1], [2], autonomous exploration [3], path planning of robotic manipulators [4], target surveillance [5], [6], collision avoidance in complex environments [7], [8], search and rescue [9], [10], and object transportation [11]. Some popular multi-vehicle coordination methods include formation control, coverage, rendezvous and containment. As one of the most effective control approaches, distributed formation control aims to coordinate a group of intelligent unmanned aerial or ground vehicles to form a desired configuration via local information. Fig. 1 depicts an application example of distributed formation control, where three quadrotors are maintaining a fixed triangle formation in a package delivery mission.

Among all the formation protocols, the majority are based on edge measurement, where the control of each unmanned vehicle relies on the relative position of its neighbors. For instance, Lin et al. [12] proposed a distributed formation law via complex Lapacian matrix. The formation protocol for double-integrator swarm system was discussed in [13]. In another study, novel formation-containment control strategies were proposed in [14] for both single and double integrator swarm robotic systems. The authors in [15] proposed a robust formation tracking protocol for networked robots considering uncertainties and disturbances. Distributed formation law for unmanned underwater vehicles was studied in [16] and this protocol is robust to disturbances and parametric uncertainties in the system. However, in aforementioned research studies, one of the constraints is that the relative position between every neighbouring robot should be detectable, which requires high quality sensors in real-world implementation. Hence, the tracking accuracy of this method may not be guaranteed in some extreme environments.

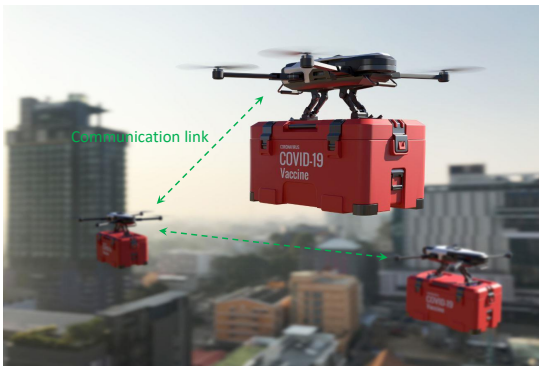

Fig. 1. A package delivery task using three networked quadrotors.

In order to deal with such limitations, many researchers have started to pay attention to the bearing-based controller, which means each vehicle just needs to measure the relative bearing of their neighbours. Compared to edge-based controller, bearing-based approaches can minimise the sensing requirements of each vehicle since the bearing signals can be detected by wireless sensor arrays [17] or vision sensors [18] in the hardware implementation. In [19] and [20], the authors discussed cyclic and triangular formations in 2-D space respectively. The bearing rigidity theory was established in [21] to characterise the properties of the target formation. Bae et al. [22] studied the converge of the bearing-only formation protocols for single-integrator MVSs with bounded exogenous disturbance. In another study, Li et al. proposed the adaptive bearing-based formation protocol for nonholonomic MVSs in [23]. Furthermore, a gradient-descent finite-time formation tracking strategy was pro-

This work was supported by EU H2020-FET-OPEN RoboRoyale project [grant number 964492], the Engineering and Physical Sciences Research Council (EPSRC) [grant number EP/W001128/1], and the Royal Academy of Engineering [grant number CiET1819].

K. Wu, B. Lennox and F. Arvin are with the Department of Electrical and Electronic Engineering, University of Manchester, Manchester, M13 9PL, U.K. (e-mail: {kefan.wu, barry.lennox, farshad.arvin}@manchester.ac.uk)

J. Hu is with the Department of Computer Science, University College London, London, WC1E 6BT, U.K. (e-mail: junyan.hu@ucl.ac.uk)

posed in [24] for heterogeneous mobile robots. Nevertheless, bearing-based approaches may lead to a slower convergence rate with the comparison of edge-based formation methods. In addition, the configuration of the formation cannot be fixed via bearing-only methods in the leaderless case.

Motivated by the advantages and limitations of both edge-based and bearing-based controllers, we propose a novel mixed formation protocol that contains both edge-based and bearing-based measurements, which helps maximise the utilisation of the sensing-ability of each unmanned vehicle. Based on the different scenarios of the formation missions, both leaderless and leader-follower cases are considered when designing the protocol and in both cases convergence of the controlled output can be guaranteed via Lyapunov theory. The main contribution of this article is as follows

- A novel mixed formation control approach with edge and bearing measurements is proposed, which can be used to maximise the tracking performance based on the sensing-ability of each unmanned vehicle in a multi-vehicle team.
- Both leaderless and leader-follower cases are considered in this paper. By using Lyapunov theory, all the unmanned vehicles can be proved to achieve the target formation asymptotically for leaderless case and exponentially for leader-follower case.

The remainder of paper is organised as follow. Section 2 introduces the relevant preliminaries and presents the main objective of the paper. In Section 3, we propose the mixed formation protocols based on edge and bearing measurements for both leaderless and leader-follower cases and analyse the stability of the MVS. Section 4 provides simulation results to validate the theoretical results and Section 5 concludes the article.

II. Preliminaries and Problem Descriptions

A. Graph Theory and Notions

Let $x_i(t) \in \mathbb{R}^p$ $(i \in \{1, 2, \cdots, n\})$ denote the state of the ith vehicle at time t, and $x(t) = [x_1(t)^\top, \cdots, x_n(t)^\top]^\top$. The interaction topology among the vehicles is denoted as $\mathcal{G} = (\mathcal{V}, \mathcal{E})$, where $\mathcal{V} = \{v_1, \ldots, v_n\}$ and $\mathcal{E} \subseteq \mathcal{V} \times \mathcal{V}$ denote the vertex and the edge set of the vehicles. We say $(i, j) \in \mathcal{E}$ if the communication can be transmitted from the ith vehicle to the jth vehicle. The adjacency matrix of $\mathcal{G}$ can be written as $\mathcal{A} = [a_{ij}] \in \mathbb{R}^{n\times n}$, where $a_{ij} > 0$ if $(i, j) \in \mathcal{E}$ and $a_{ij} = 0$, otherwise. Hence, the Laplacian matrix of $\mathcal{G}$ can be defined as $\mathcal{L} = \mathcal{D} - \mathcal{A}$, where $\mathcal{D} = diag\{d_{11}, \cdots, d_{nn}\} \in \mathbb{R}^{n\times n}$ and $d_{ii} = \sum_{j\neq i} a_{ij}$. It is obvious that $\mathcal{L}$ is positive semi-definite for undirected topology and $\mathcal{L}\mathbf{1}_n = 0$, where $\mathbf{1}_n = [1, \cdots, 1]^\top$ [25].

The related position and direction of the ith and jth vehicles can be expressed by

$$e_{ij} = x_j - x_i \ , \quad g_{ij} = \frac{e_{ij}}{\|e_{ij}\|} \ ,$$

where $\|\cdot\|$ denotes the Euclidean norm of a vector or the spectral norm of a matrix. We also call e_{ij} and g_{ij} as edge and bearing vectors respectively. Suppose there are m undirected edges in $\mathcal{G}$ and edge (i, j) is the kth edge $(k \in \{1, 2, \cdots, m\}$. The edge and bearing vectors for edge (i, j) can be redefined as $e_k = e_{ij}$ and $g_k = g_{ij}$.

The oriented graph of $\mathcal{G}$ is defined as the assignment of an orientation for all edges in $\mathcal{G}$. Define $H = [H]_{ij} \in \mathbb{R}^{m\times n}$ as the incidence matrix of the oriented graph of $\mathcal{G}$. For the kth edge (i, j), we have $[H]_{ki} = 1$ if i is the head of (i, j), $[H]_{kj} = -1$ if j is the tail of (i, j), and $[H]_{kl} = 0$ if $l \neq i, j$. Let $e = [e_1(t)^\top, \cdots, e_m(t)^\top]^\top$, we can easily find that $e = \hat{H}x$, where $\hat{H} = H \otimes I_p$, $I_p \in \mathbb{R}^{p\times p}$ denotes the identity matrix, and $\otimes$ represents the Kronecker product.

Define $\mathcal{B} = [\mathcal{B}]_{ij} \in \mathbb{R}^{pn\times pn}$ as the bearing Laplacian matrix for $\mathcal{G}$, where $[\mathcal{B}]_{ij} = g_{ij}g_{ij}^\top - I_p$ if $i \neq j$ and $(i, j) \in \mathcal{E}$, $[\mathcal{B}]_{ij} = \mathbf{0}_{\mathbf{p}\times\mathbf{p}}$ if $i \neq j$ and $(i, j) \notin \mathcal{E}$, and the diagonal entries $[\mathcal{B}]_{ii} = \sum_{j\neq i}[\mathcal{B}]_{ij}$. The bearing Laplacian matrix $\mathcal{B}$ plays a significant role in bearing-based formation control because it contains the properties of the formation.

B. Problem Descriptions

Suppose that the dynamics of the ith vehicle can be described by

$$\dot{x}_i(t) = u_i(t), \ \ i \in \{1, 2, \cdots, n\} \ , \tag{1}$$

where $u_i(t) \in \mathbb{R}^p$ denotes the control input of ith vehicle. The main problem to be solved is described as follows.

Problem: Design the formation protocols for each vehicle based on both edge vectors $\{e_{ij}\}_{j\in\mathcal{N}_i}$ and bearing vectors $\{g_{ij}\}_{j\in\mathcal{N}_i}$ such that all the vehicles will converge to the target formation x^*.

To deal with the problem, we have the following assumptions.

Assumption 1 : There exists at least one spanning tree in the interaction topology $\mathcal{G}$.

This assumption is universally used in networked formation problem since the configuration of the target formation can be guaranteed by edge vectors [25].

Assumption 2 : There is no collision during the formation task.

This assumption guarantees that the bearing vector between any pair of neighbours is always well defined during the formation construction, which has been commonly used in the bearing-based control problems such as [19], [26].

III. Edge-based and bearing-based formation controller design for multi-vehicle systems

A. Formation Protocols for Leaderless Case

In this section, we design the formation protocol for each vehicle in the leaderless case. The control input of the ith vehicle can be written as

$$u_i(t) = u_i^e(t) + u_i^b(t), \ \ i \in \{1, 2, \cdots, n\} \ , \tag{2}$$

where $u_i^e(t)$ and $u_i^b(t)$ denote the controller measured by edge vectors $\{e_{ij}\}_{j\in\mathcal{N}_i}$ and bearing vectors $\{g_{ij}\}_{j\in\mathcal{N}_i}$, which can be designed as

$$u_i^e(t) = \sum_{i\in\mathcal{N}_i} c_{ij}^e(e_{ij} - e_{ij}^*) \ , \tag{3}$$

$$u_i^b(t) = \sum_{i\in\mathcal{N}_i} c_{ij}^b(g_{ij} - g_{ij}^*) \ , \tag{4}$$

where c_{ij}^e and c_{ij}^b are positive control gains. The compact form of (2) can be written as

$$\dot{x} = -\hat{H}^\top \bar{C}_e(e - e^*) - \hat{H}^\top \bar{C}_b(g - g^*) \ , \tag{5}$$

where $\bar{C}_e = C_e \otimes I_p$ and $C_e = diag\{c_{ij}^e\}$; $\bar{C}_b = C_b \otimes I_p$ and $C_b = diag\{c_{ij}^b\}$. In order to analyse the convergence of the system (5), we have the following results

Lemma 1: For any positive-definite diagonal matrix $Q = diag\{q_1, \cdots, q_m\} \in \mathbb{R}^{m\times m}$, the following inequalities hold if Assumption 1 is satisfied

$$x^\top \hat{H}^\top \bar{Q}(g - g^*) \geq 0 \ , \tag{6}$$

$$-(x^*)^\top \hat{H}^\top \bar{Q}(g - g^*) \geq 0 \ , \tag{7}$$

where $\bar{Q} = Q \otimes I_p$. The equalities hold if and only if $g - g^* = 0$.

Proof: According to the discussion in [26, Lemma 2] and $q_k > 0, \ \forall k \in \{1, 2, \cdots, m\}$, we have

$$\begin{aligned} x^\top \hat{H}^\top \bar{Q}(g - g^*) &= \sum_{k=1}^{m} q_k \|e_k\|(1 - g_k^\top g_k^*) \\ &= \frac{1}{2}\sum_{k=1}^{m} q_k \|e_k\| \|g_k - g_k^*\| \geq 0. \end{aligned} \tag{8}$$

Similarly, we can get

$$\begin{aligned} -(x^\top)^* \hat{H}^\top \bar{Q}(g - g^*) &= \sum_{k=1}^{m} q_k \|e_k^*\|(1 - g_k^\top g_k^*) \\ &= \frac{1}{2}\sum_{k=1}^{m} q_k \|e_k^*\| \|g_k - g_k^*\| \geq 0. \end{aligned} \tag{9}$$

This completes the proof. ∎

Lemma 2: The equilibrium of system (5) satisfies $e = e^*$, that is to say $\dot{x} = 0 \Leftrightarrow e = e^*$.

Proof: Since $e = e^*$ contains $g = g^*$, the sufficient part is finished. Now, we only focus on the necessity part. By $\dot{x} = 0$, we have

$$\begin{aligned} (x - x^*)^\top \dot{x} = &-(x - x^*)\hat{H}^\top \bar{C}_b(g - g^*) \\ &- (e - e^*)^\top \bar{C}_e(e - e^*) \ . \end{aligned} \tag{10}$$

Consider that $-(e - e^*)^\top \bar{C}_e(e - e^*) \leq 0$ and the equality holds if and only if $e = e^*$. Combining with lemma 1, we have $(x - x^*)^\top \dot{x} \leq 0$ and the equality holds if $e = e^*$. Thus we complete the proof. ∎

Define the centriod of the formation as

$$\bar{x} = \frac{1}{n}\sum_{i=1}^{n} x_i = \frac{(\mathbf{1}_n \otimes I_p)x}{n},$$

where $\mathbf{1}_n = [1, 1 \cdots, 1]^\top \in \mathbb{R}^n$. The following Lemma holds.

Lemma 3: For system (2), the centriod $\bar{x}$ is fixed under the protocols (3) and (4) during the formation task.

Proof: By the definition of H, we have

$$\bar{H}(\mathbf{1}_n \otimes I_p) = H\mathbf{1}_n \otimes I_p = 0.$$

Then, we can imply that

$$\begin{aligned} \dot{\bar{x}} &= \frac{(\mathbf{1}_n \otimes I_p)\dot{x}}{n} \\ &= -\frac{(\bar{H}(\mathbf{1}_n \otimes I_p))^\top(\bar{C}_e(e - e^*) - \bar{C}_b(g - g^*))}{n} \\ &= 0. \end{aligned} \tag{11}$$

Now, we finish the proof. ∎

Next, we will analyse the stability of our formation protocols and present the following result.

Theorem 1: If we set $\bar{x}^* = \bar{x}(0)$, under Assumptions 1 and 2, all the autonomous vehicles will converge to target formation x^* asymptotically by control protocols (3) and (4).

Proof: From lemma 3, we have the centriod of the formation is fixed during the formation. Hence we can set the centriod of the target formation $\bar{x}^*$ as $\bar{x}(0)$, which is invariant. By combining with Assumption 1, we can imply that x^* can be uniquely determined by e^*. That is to say $e = e^* \Leftrightarrow x = x^*$. Let $\delta_x = x - x^*$, consider the following Lyapunov function

$$V = \frac{1}{2}\delta_x^\top \delta_x \ .$$

From lemma 2, the derivative of V can be expressed as

$$\begin{aligned} \dot{V} &= \delta_x^\top \dot{\delta}_x = \delta_x^\top \dot{x} \\ &= -\delta_x^\top \hat{H}^\top \bar{C}_b(g - g^*) - \delta_x^\top \hat{H}^\top \bar{C}_e(e - e^*) \\ &= -(x - x^*)^\top \hat{H}^\top (g - g^*) - (e - e^*)^\top C_e(e - e^*) \\ &\leq 0 \end{aligned} \tag{12}$$

and $\dot{V} = 0 \Leftrightarrow e = e^*$. Then, we can imply that the equilibrium of system (5) is stable. Hence, all the robots will converge to target formation x^* asymptotically by control protocols (3) and (4). ∎

B. Formation Protocols for Leader-follower Case

This section studies the formation protocol for leader-follower system. Suppose there are n_l stationary leaders ($\dot{x}_i = 0, \ \forall i \in \{1, 2, \cdots, n_l\}$) and n_f followers ($n_l + n_f = n$). The dynamics of the follower vehicles can be described as

$$\dot{x}_i(t) = u_i(t), \ \ i \in \{n_l + 1, n_l + 2, \cdots, n\} \ , \tag{13}$$

where the controller $u_i(t) = u_i^e(t) + u_i^b(t)$ is still measured by edge vectors $\{e_{ij}\}_{j\in\mathcal{N}_i}$ and bearing vectors $\{g_{ij}\}_{j\in\mathcal{N}_i}$.

The partition of $\mathcal{B}$ and $\mathcal{L}$ according to the leaders and followers can be expressed as

$$\mathcal{B} = \begin{bmatrix} \mathcal{B}_{ll} & \mathcal{B}_{lf} \\ \mathcal{B}_{lf}^\top & \mathcal{B}_{ff} \end{bmatrix}, \mathcal{L} = \begin{bmatrix} \mathcal{L}_{ll} & \mathcal{L}_{lf} \\ \mathcal{L}_{lf}^\top & \mathcal{L}_{ff} \end{bmatrix} \ , \tag{14}$$

where $\mathcal{B}_{ll} \in \mathbb{R}^{pn_l \times pn_l}$ and $\mathcal{B}_{ff} \in \mathbb{R}^{pn_f \times pn_f}$, $\mathcal{L}_{ll} \in \mathbb{R}^{n_l \times n_l}$ and $\mathcal{L}_{ff} \in \mathbb{R}^{n_f \times n_f}$. The following assumption is presented to ensure that the uniqueness of the target formation x^*.

Assumption 3 : The target formation x^* can be uniquely determined by the edge vectors $\{e_{ij}\}_{j\in\mathcal{N}_i}$ and the bearing vectors $\{g_{ij}\}_{j\in\mathcal{N}_i}$.

From the Lemma 1 in [26], we can easily find that Assumption 3 holds if and only if $\mathcal{B}_{ff} > 0$. It also can be obtained that $\mathcal{L}_{ff} > 0$ by Assumption 1 ([27]). To analyse the stability of our formation protocols (3) and (4), we provide the following Lemma.

Lemma 4: For any positive-definite diagonal matrix $Q = diag\{q_1, \cdots, q_m\} \in \mathbb{R}^{m\times m}$, the following inequality holds if Assumption 1 is satisfied

$$x^\top \hat{H}^\top \bar{Q}(g - g^*) \geq \frac{\tilde{q}x^\top \mathcal{B}x}{2\max_k \|e_k\|}, \tag{15}$$

where $\bar{Q} = Q \otimes I_p$ and $\tilde{q} = \min\{q_1, \cdots, q_m\}$.

Proof: From [26, Lemma 3], we can get

$$x^\top \mathcal{B}x = \sum_{k=1}^{m} \|e_k\|^2 (1 + g_k^\top g_k^*)(1 - g_k^\top g_k^*). \tag{16}$$

Since $\tilde{q} \leq q_k$, $\forall k \in \{1, \cdots, m\}$ and $1 + g_k^\top g_k^* \leq 2$, we have

$$\begin{aligned} \tilde{q}x^\top \mathcal{B}x &\leq 2\max_k \|e_k\| \sum_{k=1}^{m} \tilde{q}\|e_k\|(1 - g_k^\top g_k^*) \\ &\leq 2\max_k \|e_k\| \sum_{k=1}^{m} q_k\|e_k\|(1 - g_k^\top g_k^*) \\ &= 2\max_k \|e_k\| x^\top \hat{H}^\top \bar{Q}(g - g^*). \end{aligned} \tag{17}$$

Hence, we can imply that (15) holds. ∎

The following Theorem is presented to reveal the convergence of the protocols (3) and (4) in leader-follower case.

Theorem 2: Under Assumption 1, 2 and 3, all the vehicles will converge to target formation x^* exponentially if we apply the control protocols (3) and (4) for each follower vehicle.

Proof: Let $x_l = [x_1^\top, \cdots, x_{n_l}^\top]^\top$ and $x_f = [x_{n_l+1}^\top, \cdots, x_n^\top]^\top$ denote the state of the leaders and followers, and $x = [x_l^\top, x_f^\top]^\top$. Substituting (3) and (4) into (13), the compact form of (13) can be rewritten as

$$\dot{x} = -\Gamma \bar{C}_e \hat{H}^\top (e - e^*) - \Gamma \bar{C}_b \hat{H}^\top (g - g^*), \tag{18}$$

where $\Gamma = \begin{bmatrix} 0 & 0 \\ 0 & I_{pn_f} \end{bmatrix}$.

Let $\delta_x = x(t) - x^* = [0, \delta_{x_f}^\top]^\top$, we can imply that $\delta_x \Gamma = \delta_x$ because the leaders are fixed. Consider the following Lyapunov function candidate,

$$V = \frac{1}{2}\delta_x^\top \delta_x .$$

According to (6) and (12), the derivative of V is shown as

$$\begin{aligned} \dot{V} &= \delta_x^\top \dot{\delta}_x = \delta_x^\top \dot{x} \\ &= -\delta_x^\top \Gamma \hat{H}^\top \bar{C}_b (g - g^*) - \delta_x^\top \Gamma \hat{H}^\top \bar{C}_e (e - e^*) \\ &= -\delta_x^\top \hat{H}^\top \bar{C}_b (g - g^*) - \delta_x^\top \hat{H}^\top \bar{C}_e (e - e^*) \\ &\leq -x^\top \hat{H}^\top \bar{C}_b (g - g^*) - \delta_x^\top \hat{H}^\top \bar{C}_e \hat{H} \delta_x \\ &= -x^\top \hat{H}^\top \bar{C}_b (g - g^*) - \delta_x^\top \hat{\mathcal{L}} \delta_x \\ &\leq 0 \end{aligned} \tag{19}$$

where $\hat{\mathcal{L}} = \mathcal{L} \otimes I_p$. We can conclude that $\mathcal{B}x^* = 0$ from the definition of $\mathcal{B}$. Let $\hat{\mathcal{L}}_{ff} = \mathcal{L}_{ff} \otimes I_p$, then, by Lemma 4, it follows that

$$\begin{aligned} \dot{V} &\leq -\frac{\tilde{q}x^\top \mathcal{B}x}{2\max_k \|e_k\|} - \delta_{x_f}^\top \hat{\mathcal{L}}_{ff} \delta_{x_f} \\ &\leq -\frac{\tilde{q}\delta_x^\top \mathcal{B}\delta_x}{2\max_k \|e_k\|} - \delta_{x_f}^\top \hat{\mathcal{L}}_{ff} \delta_{x_f} \\ &= -\frac{\tilde{q}\delta_{x_f}^\top \mathcal{B}_{ff}\delta_{x_f}}{2\max_k \|e_k\|} - \delta_{x_f}^\top \hat{\mathcal{L}}_{ff} \delta_{x_f} \\ &\leq -(\frac{\tilde{q}\lambda_{\min}(\mathcal{B}_{ff})}{2\|e\|} + \lambda_{\min}(\hat{\mathcal{L}}_{ff}))\|\delta_x\|^2. \end{aligned} \tag{20}$$

From (12), we can indicate that $\delta_x(t) \leq \delta_x(0)$. Hence we can get

$$\begin{aligned} \|e\| &\leq \|\hat{H}\|\|x\| = \|\hat{H}\|\|x^* + \delta_x\| \\ &\leq \|\hat{H}\|(\|x^*\| + \|\delta_x\|) \\ &\leq \|\hat{H}\|(\|x^*\| + \|\delta_x(0)\|). \end{aligned} \tag{21}$$

This together with (20), we have

$$\begin{aligned} \dot{V} &\leq -(\frac{\tilde{q}\lambda_{\min}(\mathcal{B}_{ff})}{\|\hat{H}\|(\|x^*\| + \|\delta_x(0)\|)} + 2\lambda_{\min}(\hat{\mathcal{L}}_{ff}))V \\ &= -\alpha V. \end{aligned} \tag{22}$$

That is to say that all the vehicles will converge to target formation x^* exponentially with the exponential convergence rate $\alpha = \frac{\tilde{q}\lambda_{\min}(\mathcal{B}_{ff})}{\|\hat{H}\|(\|x^*\| + \|\delta_x(0)\|)} + 2\lambda_{\min}(\hat{\mathcal{L}}_{ff})$. ∎

Remark 1: The control gains c_i^e and c_i^b represent the weights of the edge-based and bearing-based control effort. To deal with the sensors with low quality, the edge-based gain c_i^e could be selected smaller and the bearing-based gain c_i^b could be selected larger to reduce the affect of low accuracy measured by positions.

IV. Simulation Results

In this section, the performance of the formation protocols (3) and (4) is verified by MATLAB for both leaderless and leader-follower cases.

A. Simulation Case Study without Leaders

In this simulation, six mobile robots are deployed for the leaderless case. We set the shape of the target formation as a regular hexagon (linked by red solid lines in Fig 2). The control gains c_{ij}^e and c_{ij}^b are selected randomly from $(0, 1)$ and satisfy $c_{ij}^e + c_{ij}^b = 1$. In Fig 2, the initial positions of six robots (denoted by six different colours) are linked by blue dashed lines. Hence, we can calculate the centroid $\bar{x}(0)$, which will be set as the centroid of the target formation (denoted by the yellow star). The trajectories of six robots are shown by dashed lines with six different colours corresponding to each robot. Fig 3(a) and 3(b) show the control inputs of the six robots along the x-axis (u_x) and y-axis (u_y) during the task. In Fig 4, we can see that the bearing error ($\|g - g^*\|$), edge error ($\|e - e^*\|$) and the statement error ($\|x - x^*\|$) converge to zero within 15 seconds. It can be observed from these results that the control protocols (3) and (4) are effective at accomplishing the formation task.

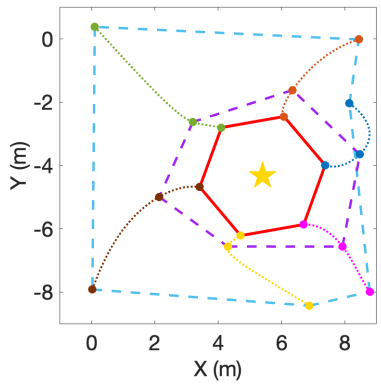

Fig. 2. Trajectories of the six robots with a fixed centroid (yellow star).

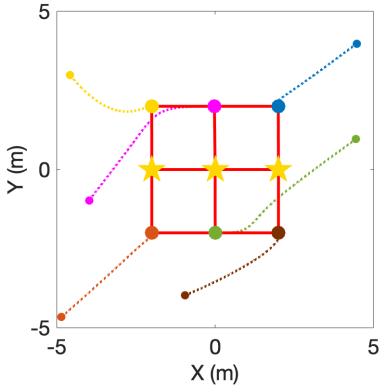

Fig. 5. Trajectories of six follower robots with fixed leaders (yellow stars).

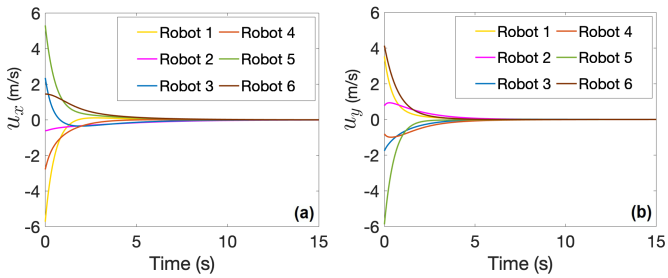

Fig. 3. Control inputs of the six robots. (a) Along the X-axis (u_x). (b) Along the Y-axis (u_y).

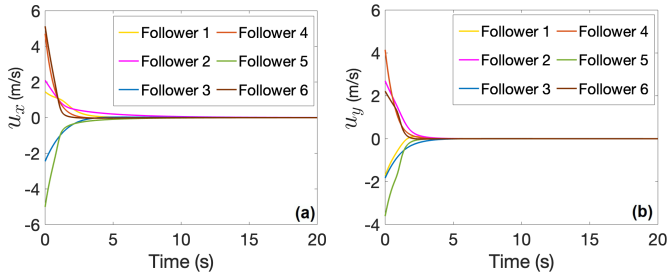

Fig. 6. Control inputs of six follower robots. (a) Along the X-axis (u_x). (b) Along the Y-axis (u_y).

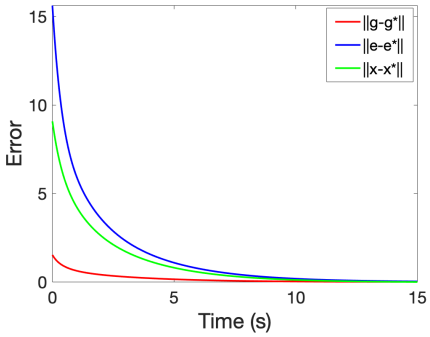

Fig. 4. Time variation of the bearing error ($\|g-g^*\|$), edge error ($\|e-e^*\|$), and state error ($\|x-x^*\|$).

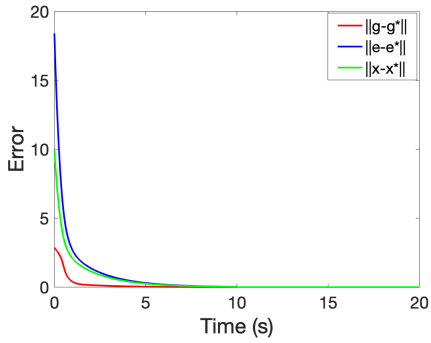

Fig. 7. Time variation of the bearing error ($\|g-g^*\|$), edge error ($\|e-e^*\|$), and state error ($\|x-x^*\|$).

B. Simulation Case Study with Leaders

In this simulation, nine mobile robots (six followers and three stationary leaders) are deployed for the leader-follower case. The shape of the target formation is selected as four small squares, together with a large square (linked by red solid lines in Fig 5). We choose the control gains c_{ij}^e and c_{ij}^b randomly from $(0, 1)$ and satisfy $c_{ij}^e + c_{ij}^b = 1$. In Fig 5, the initial positions of three leaders (denoted by three yellow stars) are $[-2, 0]$, $[0, 0]$, and $[2, 0]$. The yellow, pink, blue, brown, green, and orange dashed lines denote the trajectories of six follower robots from their initial states to target formation. The control inputs of six follower vehicles along the x-axis (u_x) and y-axis (u_y) are shown in Fig 6(a) and Fig 6(b), respectively. In Fig 7, we can see that the bearing error ($\|g - g^*\|$), edge error ($\|e - e^*\|$) and the statement error ($\|x - x^*\|$) converges to zero. Hence, the control objective can be fulfilled under the proposed mixed formation protocol.

C. Comparison with Bearing-Only Protocol

To demonstrate the superior performance of the proposed mixed strategy, we make a comparison of the proposed controller with the bearing-only protocol proposed in [26]. For this comparison, nine mobile robots including six followers and three stationary leaders were deployed. We adopted the same target formation and the initial positions of three leaders in Section IV.B and ran 50 simulations for each controller with the initial positions of each follower chosen randomly from $[-4, 4] \times [-4, 4]$. The performances of the mixed and

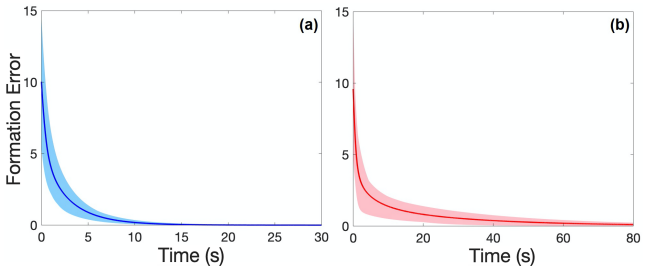

Fig. 8. Controller performance of (a) mixed protocol, (b) bearing-only protocol.

bearing-only protocols are displayed in Fig. 8(a) and 8(b), respectively. We utilize $\|x-x^*\|$ to define the formation error. The blue and red zones illustrate the results of 50 simulations and the dark blue and red solid lines represent the average result of the mixed protocol and bearing-only protocol. It can be concluded from the comparison that the convergence time of the mixed protocol ($T = 20$s) is shorter then the bearing-only protocol ($T = 80$s). Hence, the proposed mixed protocol can be used to increase the convergence rate of the formation and maximise the tracking performance based on the sensing-ability of each robot.

V. Conclusion

A novel mixed formation controller for multi-vehicle systems (MVSs) was proposed in this paper via both edge-based and bearing-based measurements. Both leaderless and leader-follower cases were considered in the protocol design. The stability of the MVSs can be guaranteed by choosing an appropriate Lyapunov function. Finally, the simulation results were demonstrated to validate the effectiveness of the proposed formation protocols.

In the future, hardware experiments using unmanned aerial vehicles (as followers) and unmanned ground vehicles (as the leaders) will be conducted to verify the feasibility of the theoretical results in real-world scenarios. Furthermore, the nonlinear dynamics of the vehicles and time-delays of the communication networks will be considered in the protocol design.

References

[1] G. Di Mauro, M. Lawn, and R. Bevilacqua, "Survey on guidance navigation and control requirements for spacecraft formation-flying missions," *Journal of Guidance, Control, and Dynamics*, vol. 41, no. 3, pp. 581–602, 2018.

[2] J. Hu, H. Niu, J. Carrasco, B. Lennox, and F. Arvin, "Fault-tolerant cooperative navigation of networked UAV swarms for forest fire monitoring," *Aerospace Science and Technology*, 2022.

[3] M. Corah and N. Michael, "Distributed matroid-constrained submodular maximization for multi-robot exploration: Theory and practice," *Autonomous Robots*, vol. 43, no. 2, pp. 485–501, 2019.

[4] W. Liu, H. Niu, M. N. Mahyuddin, G. Herrmann, and J. Carrasco, "A model-free deep reinforcement learning approach for robotic manipulators path planning," in *2021 21st International Conference on Control, Automation and Systems (ICCAS)*. IEEE, 2021, pp. 512–517.

[5] J. Hu, A. E. Turgut, B. Lennox, and F. Arvin, "Robust formation coordination of robot swarms with nonlinear dynamics and unknown disturbances: Design and experiments," *IEEE Transactions on Circuits and Systems II: Express Briefs*, vol. 69, no. 1, pp. 114–118, 2022.

[6] T. Li, H.-S. Shin, and A. Tsourdos, "Efficient decentralized task allocation for uav swarms in multi-target surveillance missions," in *2019 International Conference on Unmanned Aircraft Systems (ICUAS)*. IEEE, 2019, pp. 61–68.

[7] S. Na, H. Niu, B. Lennox, and F. Arvin, "Bio-inspired collision avoidance in swarm systems via deep reinforcement learning," *IEEE Transactions on Vehicular Technology*, 2022.

[8] H. Niu, Z. Ji, F. Arvin, B. Lennox, H. Yin, and J. Carrasco, "Accelerated sim-to-real deep reinforcement learning: Learning collision avoidance from human player," in *2021 IEEE/SICE International Symposium on System Integration (SII)*. IEEE, 2021, pp. 144–149.

[9] J. Hu, P. Bhowmick, I. Jang, F. Arvin, and A. Lanzon, "A decentralized cluster formation containment framework for multirobot systems," *IEEE Transactions on Robotics*, vol. 37, no. 6, pp. 1936–1955, 2021.

[10] F. Niroui, K. Zhang, Z. Kashino, and G. Nejat, "Deep reinforcement learning robot for search and rescue applications: Exploration in unknown cluttered environments," *IEEE Robotics and Automation Letters*, vol. 4, no. 2, pp. 610–617, 2019.

[11] J. Hu, P. Bhowmick, and A. Lanzon, "Group coordinated control of networked mobile robots with applications to object transportation," *IEEE Transactions on Vehicular Technology*, vol. 70, no. 8, pp. 8269–8274, 2021.

[12] Z. Lin, L. Wang, Z. Han, and M. Fu, "Distributed formation control of multi-agent systems using complex laplacian," *IEEE Transactions on Automatic Control*, vol. 59, no. 7, pp. 1765–1777, 2014.

[13] X. Dong, B. Yu, Z. Shi, and Y. Zhong, "Time-varying formation control for unmanned aerial vehicles: Theories and applications," *IEEE Transactions on Control Systems Technology*, vol. 23, no. 1, pp. 340–348, 2014.

[14] K. Wu, J. Hu, B. Lennox, and F. Arvin, "Sdp-based robust formation-containment coordination of swarm robotic systems with input saturation," *Journal of Intelligent & Robotic Systems*, vol. 102, no. 1, 2021.

[15] J. Hu, B. Lennox, and F. Arvin, "Robust formation control for networked robotic systems using negative imaginary dynamics," *Automatica*, 2022.

[16] H. Liu, Y. Wang, and F. L. Lewis, "Robust distributed formation controller design for a group of unmanned underwater vehicles," *IEEE Transactions on Systems, Man, and Cybernetics: Systems*, 2019.

[17] R. Tron, J. Thomas, G. Loianno, K. Daniilidis, and V. Kumar, "A distributed optimization framework for localization and formation control: Applications to vision-based measurements," *IEEE Control Systems Magazine*, vol. 36, no. 4, pp. 22–44, 2016.

[18] G. Mao, B. Fidan, and B. D. Anderson, "Wireless sensor network localization techniques," *Computer Networks*, vol. 51, no. 10, pp. 2529–2553, 2007.

[19] S. Zhao and D. Zelazo, "Bearing rigidity and almost global bearing-only formation stabilization," *IEEE Transactions on Automatic Control*, vol. 61, no. 5, pp. 1255–1268, 2015.

[20] M. Basiri, A. N. Bishop, and P. Jensfelt, "Distributed control of triangular formations with angle-only constraints," *Systems & Control Letters*, vol. 59, no. 2, pp. 147–154, 2010.

[21] S. Zhao and D. Zelazo, "Localizability and distributed protocols for bearing-based network localization in arbitrary dimensions," *Automatica*, vol. 69, pp. 334–341, 2016.

[22] Y.-B. Bae, H.-S. Ahn, and Y.-H. Lim, "Leader-follower bearing-based formation system with exogenous disturbance," in *2019 IEEE 13th International Symposium on Applied Computational Intelligence and Informatics (SACI)*. IEEE, 2019, pp. 000 039–000 044.

[23] X. Li, C. Wen, X. Fang, and J. Wang, "Adaptive bearing-only formation tracking control for nonholonomic multiagent systems," *IEEE Transactions on Cybernetics*, 2021.

[24] K. Wu, J. Hu, B. Lennox, and F. Arvin, "Finite-time bearing-only formation tracking of heterogeneous mobile robots with collision avoidance," *IEEE Transactions on Circuits and Systems II: Express Briefs*, 2021.

[25] C. Godsil and G. F. Royle, *Algebraic graph theory*. Springer Science & Business Media, 2013, vol. 207.

[26] S. Zhao, Z. Li, and Z. Ding, "Bearing-only formation tracking control of multiagent systems," *IEEE Transactions on Automatic Control*, vol. 64, no. 11, pp. 4541–4554, 2019.

[27] Z. Meng, W. Ren, and Z. You, "Distributed finite-time attitude containment control for multiple rigid bodies," *Automatica*, vol. 46, no. 12, pp. 2092–2099, 2010.